axioms

MDPI

Article

Estimator-Based Time-Varying Feedback Control for Uncertain, Anti-Stable Heat Equation in a Prescribed Finite Time

Chengzhou Wei

School of Artificial Intelligence, Taizhou University, Taizhou 318000, China; czwei@tzc.edu.cn

Abstract

This paper studies prescribed-time (PT) stabilization for a heat equation with an unstable term at the uncontrolled boundary, subject to external disturbances and internal unknown mode uncertainties at the controlled boundary. A boundary time-varying output feedback control scheme based on disturbance estimation is developed, where the convergence time is independent of the initial condition and can be specified a priori. A disturbance estimator using boundary measurements and a time-varying tuning function enables prescribed-time estimation of both the disturbance and the system state. By integrating active disturbance rejection control with the backstepping technique, a boundary output feedback controller is derived. A simulation example from the burning process of a solid propellant rocket demonstrates the effectiveness of the proposed approach.

Keywords: heat equation; disturbance estimator; prescribed-time stabilization; time-varying feedback; backstepping approach

MSC: 93B52; 93D15; 93D09

1. Introduction

The control of distributed parameter systems governed by partial differential equations (PDEs) has attracted considerable attention in recent years due to its wide range of engineering applications [1–3]. In this paper, we consider an uncertain anti-stable heat equation that arises from a linearized model of unstable burning in solid propellant rockets (see [4,5]). The system is described by

$$u_t(x,t) = u_{xx}(x,t) + \varrho e^{\alpha x} u(0,t), \quad x \in (0,1),\ t \in [0,T), \tag{1}$$

subject to the boundary conditions

$$u_x(0,t) = -qu(0,t), \quad u(1,t) = U(t) + \chi(u(\cdot,t)) + d(t), \tag{2}$$

and the initial condition

$$u(x,0) = u_0(x). \tag{3}$$

Here, ϱ, α, q are constants. The system state $u : [0,1] \times [0,T) \to \mathbb{R}$ represents the temperature distribution, and $T > 0$ denotes the prescribed terminal time. The signal $U(t)$ is the boundary control input. The term $\chi(u(\cdot,t))$ denotes internal model uncertainty,

Check for updates

Academic Editor: Valery Y. Glizer

Received: 21 January 2026
Revised: 19 March 2026
Accepted: 30 March 2026
Published: 1 April 2026

Copyright: © 2026 by the author. Licensee MDPI, Basel, Switzerland. This article is an open access article distributed under the terms and conditions of the Creative Commons Attribution (CC BY) license.

where χ may be a nonlinear mapping, and $d(t)$ represents an external disturbance. For convenience, define the total disturbance

$$D(t) := \chi(u(\cdot, t)) + d(t).$$

Further details of the physical model are provided in Remark 1.

1.1. Motivation and Objective

The control of combustion instabilities in solid propellant rockets is a critical problem in aerospace engineering. As shown in [4,5], temperature dynamics in the propellant can be modeled by an anti-stable heat equation with destabilizing boundary effects at the burning surface. If uncontrolled, such instabilities may lead to severe pressure oscillations and excessive heat transfer, which may ultimately cause engine failure.

Although exponential stabilization has been investigated in previous studies [5–9], many practical applications—such as tactical missile guidance or launch vehicle boosters—require the system to reach the desired operating condition within a strictly limited time interval independent of the initial state. Moreover, practical systems are inevitably subject to disturbances and modeling uncertainties, which calls for robust control strategies.

Motivated by these considerations, the objective of this paper is to design a boundary controller $U(t)$ such that the system state $u(x, t)$ converges to zero within a prescribed finite time T. The prescribed time T is independent of the initial condition $u_0(x)$ and can be specified a priori. In addition, only boundary measurements are assumed to be available, namely

$$y_{out}(t) = \{u(0, t), u_x(1, t)\}.$$

1.2. Methods of Dealing with Disturbance and Uncertainties

Various approaches have been proposed to handle disturbances and uncertainties, including sliding mode control (SMC), the internal model principle, adaptive control, and active disturbance rejection control (ADRC). Due to its inherent robustness to disturbances, SMC has been widely used in control design [2]. For the specific case of (1)–(3) with $g = 0$, a discontinuous robust controller was proposed in [6] by combining the backstepping approach [10] with unit SMC [11]. A related problem was studied in [7], where the unstable term $-qu(0, t)$ is absent and the resulting controller is continuous, thus avoiding the chattering phenomenon. The state feedback stabilization results in [6,7] were later extended to output feedback stabilization in [8,12] by introducing symbolic functions to construct state observers.

Adaptive control methods have also been employed to cope with parameter uncertainties [13]. When the parameters ϱ and q are unknown in (1)–(3) without boundary disturbance $D(t)$, output feedback stabilization was achieved in [14], where adaptive update laws for ϱ and q were developed based on boundary measurements. Further details can be found in the monograph [15].

For the case $\alpha = 0$, $q = 0$, and $\chi(u(\cdot, t)) = 0$, assuming that the parameter g and the upper bound of the disturbance $d(t)$ are known, ref. [9] studied output feedback stabilization by designing a frequency-domain filter to estimate the disturbance. This result was further extended in [16] to the case of unknown parameter ϱ, where the disturbance $d(t)$ is required to be differentiable.

Another effective approach is the ADRC framework proposed in [17]. The work [6] extended ADRC techniques to PDE systems by transforming the PDE into an ODE using a specific test function. However, this approach requires both $d(t)$ and its derivative $\dot{d}(t)$ to be bounded, and the disturbance estimator relies on high-gain techniques. When internal

uncertainties such as $\chi(u(\cdot,t))$ are present, these methods may become less effective. For the case $\varrho = 0$ with both $\chi(u(\cdot,t))$ and $d(t)$, ref. [18] proposed a robust output feedback controller based on an ADRC framework and a newly designed extended state observer.

1.3. Results of Finite-Time Stabilization

The results discussed above mainly guarantee exponential stabilization. However, finite-time stabilization is often desirable in practice. Extending the fractional power feedback technique for ODE systems proposed in [19] to PDE systems [20], finite-time stabilization can be achieved using Lyapunov inequalities of the form

$$\dot{V}(t) \leq -kV(t)^{\delta},$$

where $k > 0$ and $0 < \delta < 1$, $V(t)$ is the Lyapunov function, often taken as L^2 norm of the system state (see, e.g., [21–25]). In this case, the settling time depends on the initial value of the Lyapunov function. Consequently, the settling time may become arbitrarily large when the initial state is large.

To address this limitation, the concept of fixed-time stabilization was introduced in [26–29]. Although fixed-time stabilization removes the dependence on the initial state, the convergence time is generally difficult to specify explicitly. Therefore, stabilization schemes with convergence time independent of the initial condition and explicitly assignable a priori are of particular interest. This notion is commonly referred to as PT stabilization [30–45].

Recently, PT stabilization for ODE systems was investigated in [30] by introducing a time-varying gain function that diverges as time approaches the prescribed terminal time. By incorporating such a time-varying function into the backstepping design, PT stabilization for heat equations was established in [31]. Further developments can be found in [34–42,46]. However, most of these works consider disturbance-free systems. The PT stabilization of systems such as (1)–(3) in the presence of disturbances and uncertainties remains a challenging problem.

The present work differs from the related literature in three main aspects.

First, the system model differs from that considered in [41], which studies the standard heat equation with boundary disturbance. In contrast, the model considered here involves an anti-stable heat equation containing the coupling term $\rho e^{\alpha x} u(0,t)$, which arises from pressure-coupled combustion effects in solid propellant rockets. This destabilizing coupling significantly alters the system dynamics and requires a different control design.

Second, the disturbance model is more general. The disturbance is described by $\chi(u(\cdot,t)) + d(t)$, where $\chi(u(\cdot,t))$ represents a nonlinear uncertainty depending on the system state. This introduces additional coupling between the internal dynamics and the boundary input, whereas [41] considers only a boundary disturbance.

Third, an output feedback framework integrating anti-stable compensation, PT control, and disturbance estimation is developed using only the boundary measurements $u(0,t)$ and $u_x(1,t)$. In contrast, refs. [42,46] consider disturbance-free systems, while related works such as [28,38,40] require full-state feedback. The proposed approach achieves PT stabilization in the presence of disturbances using limited boundary measurements.

1.4. Contributions

The novelty of this paper lies in establishing a PT disturbance estimation method and an output feedback stabilization strategy for a heat equation involving anti-stable dynamics, boundary disturbances, and internal model uncertainties. The main contributions are summarized as follows.

1. A PT disturbance estimation framework is proposed for a class of anti-stable heat equations with boundary disturbances and internal nonlinear uncertainties. The considered model generalizes those in [6–9,12,16,18] by allowing both external disturbances and state-dependent uncertainties at the controlled boundary.
2. Based on the proposed estimator, a boundary output feedback control law is constructed using only two boundary measurements $u(0,t)$ and $u_x(1,t)$. Compared with the observer-based design in [18], the proposed approach directly utilizes the disturbance estimator and avoids constructing an additional state observer.
3. Compared with existing PT stabilization results [28,31,38,40] with state feedback, [35,42,46] with output feedback, the proposed boundary output feedback control is robust to matched boundary disturbance, while the boundary disturbance is not considered in [31,35,42,46].

1.5. Main Technical Idea

The key idea of this work is motivated by two observations. First, the instability of the system originates from the burning-end boundary, where unknown disturbances also enter the system. Since these disturbances cannot be measured directly, it is natural to reconstruct them from available boundary measurements. This leads to the introduction of a disturbance estimator, which acts as a virtual sensor for the unknown boundary disturbance.

Second, classical backstepping designs typically guarantee only exponential stabilization. To achieve convergence within a user-specified time, we incorporate time-varying gains into the backstepping framework so that the effective damping of the target system increases as the prescribed time approaches. By combining the disturbance estimator with this time-varying backstepping controller, the resulting output feedback law ensures PT stabilization of the closed-loop system.

Notation: Let $L^2([0,1];\mathbb{R})$ denote the Hilbert space of square-integrable scalar functions $u:[0,1]\to\mathbb{R}$, equipped with the norm $\|u\|^2_{L^2([0,1];\mathbb{R})}=\int_0^1 u^2(x)\,\mathrm{d}x$. Let $L^\infty([0,1];\mathbb{R})$ denote the space of essentially bounded functions on $[0,1]$, with norm $\|u\|_{L^\infty([0,1];\mathbb{R})}=\operatorname{ess\,sup}_{x\in[0,1]}|u(x)|$. For simplicity, the notations $L^2([0,1])$ and $L^\infty([0,1])$ are used when no confusion arises.

The functions $I_n(\cdot)$ and $J_n(\cdot)$ denote the modified Bessel function and the Bessel function of order n, respectively. The Gamma function is denoted by $\Gamma(\cdot)$, and $L_n^1(\cdot)$ denotes the generalized Laguerre polynomial of degree n with parameter $\alpha=1$, see [47]. The functions $\sinh(\cdot)$ and $\cosh(\cdot)$ denote the hyperbolic sine and cosine functions, respectively. Throughout the paper, $c_1>0$ denotes a generic positive constant, whose value may vary from line to line.

The paper is organized as follows. Section 2 presents the necessary lemmas. Section 3 develops the main results, including the construction of the disturbance observer, the controller design, and the closed-loop stability analysis. Section 4 provides a simulation example. The Appendix A contains the proofs related to the disturbance observer design.

Remark 1. *The temperature dynamics of a solid propellant rocket can be described by the classical Denison–Baum combustion model [48]. In this model, the distributed term $\rho e^{\alpha x}u(0,t)$ captures the pressure-coupled combustion response, through which fluctuations in the surface temperature at the burning interface influence the internal temperature field. The exponential factor $e^{\alpha x}$ characterizes the spatial attenuation of this effect along the propellant grain, while the parameters ρ and α depend on the propellant properties and operating conditions.*

The boundary condition at the burning surface $x=0$ is derived from an energy balance between the solid propellant and the gas phase. Specifically, the heat flux follows an Arrhenius-type

vaporization law, leading to a nonlinear Robin boundary condition $u_x(0,t) = -f_2(u(0,t))$. For stability analysis around an equilibrium, this nonlinear relation is linearized as $u_x(0,t) = -qu(0,t)$, where q is the corresponding linearized combustion response coefficient.

2. Preliminaries

This section introduces a technical lemma that will be used to establish the well-posedness of the system and facilitate the subsequent stability analysis. Following [34,35], consider the time-varying function

$$c(t) = \frac{\mu_0}{\nu^2(t)}, \quad \nu(t) = \frac{T-t}{T}, \quad \mu_0 > 0, \tag{4}$$

where T is the prescribed terminal time. We extend the well-posedness and stability results for heat equations with time-varying damping (see, e.g., [34,35]) to the case with a non-homogeneous boundary condition. The proof follows similar arguments, with additional treatment of the boundary input $\varpi(t)$. Let the state space be $\mathcal{H} := L^2([0,1];\mathbb{R})$.

Lemma 1. *Consider the system*

$$\begin{cases} \hat{\vartheta}_t(x,t) = \hat{\vartheta}_{xx}(x,t) - c(t)\hat{\vartheta}(x,t), \\ \hat{\vartheta}_x(0,t) = 0, \quad \hat{\vartheta}_x(1,t) = \varpi(t), \\ \hat{\vartheta}(x,0) = \hat{\vartheta}_0(x). \end{cases} \tag{5}$$

For any initial value $\hat{\vartheta}_0 \in \mathcal{H}$, the following statements hold:

(i) If $\varpi(t) \in L^2([0,T^*])$ for some $T^* < T$, then system (5) admits a solution $\hat{\vartheta} \in C([0,T);\mathcal{H})$.

(ii) The following L^2-estimate holds:

$$\|\hat{\vartheta}(\cdot,t)\|_{\mathcal{H}}^2 \le c_1 e^{\frac{-2\mu_0 T}{\nu(t)}} \|\hat{\vartheta}_0\|_{\mathcal{H}}^2 + c_1 e^{\frac{-2\mu_0 T}{\nu(t)}} \int_0^t \left(e^{\int_0^s c(\tau)\,\mathrm{d}\tau}\varpi(s)\right)^2 \mathrm{d}s. \tag{6}$$

Proof. (i) Since $c(t)$ is time-varying and has a singularity only at $t = T$, consider the transformation

$$\tilde{\vartheta}(x,t) = e^{\int_0^t c(\tau)\,\mathrm{d}\tau}\hat{\vartheta}(x,t), \tag{7}$$

which converts (5) into

$$\begin{cases} \tilde{\vartheta}_t(x,t) = \tilde{\vartheta}_{xx}(x,t), \\ \tilde{\vartheta}_x(0,t) = 0, \quad \tilde{\vartheta}_x(1,t) = e^{\int_0^t c(\tau)\,\mathrm{d}\tau}\varpi(t), \\ \tilde{\vartheta}(x,0) = \hat{\vartheta}_0(x). \end{cases} \tag{8}$$

Since $e^{\int_0^t c(\tau)\,\mathrm{d}\tau}$ is bounded on $[0,T^*]$ and $\varpi \in L^2([0,T^*])$, it follows that $e^{\int_0^t c(\tau)\,\mathrm{d}\tau}\varpi(t) \in L^2([0,T^*])$. The well-posedness of (8) then follows from [18]. As the transformation (7) is bounded and invertible on $[0,T^*]$, the well-posedness of (5) holds on $[0,T)$, yielding $\hat{\vartheta} \in C([0,T);\mathcal{H})$.

(ii) Consider the Lyapunov functional $V(t) = \frac{1}{2}\|\hat{\vartheta}(\cdot,t)\|_{\mathcal{H}}^2$. Along the solution of (5), one obtains

$$\frac{\mathrm{d}}{\mathrm{d}t}\|\hat{\vartheta}(\cdot,t)\|_{\mathcal{H}}^2 \le -2c(t)\|\hat{\vartheta}(\cdot,t)\|_{\mathcal{H}}^2 + \varpi^2(t). \tag{9}$$

Using the Poincaré inequality (see, e.g., [10]), one derives (6). This completes the proof. □

3. Main Results

The active disturbance rejection control (ADRC) method is adopted to handle the general disturbance $D(t)$. The main idea is to estimate the disturbance and compensate it in the feedback loop [17]. Moreover, the disturbance $D(t)$ is estimated within a prescribed finite time T, from which a state estimate is also obtained. Based on this estimator, a boundary output feedback controller is subsequently developed.

For notational simplicity, the dependence of functions on the spatial variable x and time variable t is omitted whenever no ambiguity arises. For example, $\vartheta(x,t)$, $\eta(x,t)$, and $\zeta(x,y,t)$ are written as ϑ, η, and $\zeta(x,y)$, respectively.

3.1. Disturbance Estimator

The control system (1)–(3) is decomposed into a known part and an unknown part, corresponding to (10) and (11), respectively, and an estimator is constructed for the unknown component.

From (2), the control input $U(t)$ and the boundary disturbance $D(t)$ enter through the same channel. To separate them, introduce the auxiliary system

$$\begin{cases} \phi_t(x,t) = \phi_{xx}(x,t) + \varrho e^{\alpha x} u(0,t), \\ \phi_x(0,t) = -qu(0,t), \quad \phi(1,t) = U(t), \\ \phi(x,0) = \phi_0(x), \end{cases} \tag{10}$$

where $\phi_0(x)$ is arbitrary. System (10) depends only on measurable signals and known inputs, and is therefore known.

Define $\hat{\phi} = u - \phi$. Then, $\hat{\phi}$ satisfies

$$\begin{cases} \hat{\phi}_t = \hat{\phi}_{xx}, \\ \hat{\phi}_x(0,t) = 0, \quad \hat{\phi}(1,t) = D(t), \\ \hat{\phi}(x,0) = \hat{\phi}_0(x), \end{cases} \tag{11}$$

which isolates the disturbance $D(t)$ at the boundary $x = 1$.

Based on (11), construct the estimator system

$$\begin{cases} \varphi_t = \varphi_{xx} + p_1(x,t)\big(\hat{\phi}(0,t) - \varphi(0,t)\big), \\ \varphi_x(0,t) = -p_2(t)\big(\hat{\phi}(0,t) - \varphi(0,t)\big), \\ \varphi_x(1,t) = u_x(1,t) - \phi_x(1,t), \\ \varphi(x,0) = \varphi_0(x), \end{cases} \tag{12}$$

where the time-varying gains $p_1(x,t)$ and $p_2(t)$ are introduced to achieve PT estimation.

For the time-invariant case (i.e., $p_1(x)$ and constant p_2), only exponential estimation can be achieved as in [18], which requires $t \to \infty$. To achieve PT estimation, we next determine $p_1(x,t)$ and $p_2(t)$.

Let $\tilde{\phi} = \hat{\phi} - \varphi$. Then,

$$\begin{cases} \tilde{\phi}_t = \tilde{\phi}_{xx} - p_1(x,t)\tilde{\phi}(0,t), \\ \tilde{\phi}_x(0,t) = p_2(t)\tilde{\phi}(0,t), \quad \tilde{\phi}_x(1,t) = 0, \\ \tilde{\phi}(x,0) = \tilde{\phi}_0(x). \end{cases} \tag{13}$$

Following [36], introduce the backstepping transformation

$$\begin{aligned}\tilde{\phi}(x,t) &= \eta(x,t) - \int_0^x \zeta(x,y,t)\eta(y,t)\,\mathrm{d}y \\ &:= [(I-\mathcal{R})\eta](x,t).\end{aligned} \tag{14}$$

Substituting (14) into (13), one verifies that if

$$\begin{cases} \zeta_{xx} - \zeta_{yy} = \zeta_t - c(t)\zeta, \\ \zeta(x,x,t) = \frac{1}{2}c(t)(x-1), \\ \zeta_x(1,y,t) = 0, \end{cases} \tag{15}$$

and

$$p_1(x,t) = \zeta_y(x,0,t), \quad p_2(t) = -\zeta(0,0,t),$$

then the target system becomes

$$\begin{cases} \eta_t = \eta_{xx} - c(t)\eta, \\ \eta_x(0,t) = 0, \quad \eta_x(1,t) = 0, \\ \eta(x,0) = \eta_0(x). \end{cases} \tag{16}$$

Lemma 2 provides the explicit expression of the kernel $\zeta(x,y,t)$, from which the gains $p_1(x,t)$ and $p_2(t)$ are explicitly determined.

Lemma 2. *The kernel function ζ in the transformation (14) is given by*

$$\zeta(x,y,t) = -(1-y)c(t)e^{\frac{-(x-y)(2-x-y)}{4Tv(t)}} \frac{I_1\left(\sqrt{c(t)(x-y)(2-x-y)}\right)}{\sqrt{c(t)(x-y)(2-x-y)}}. \tag{17}$$

$$p_1(x,t) = \zeta_y(x,0,t) = c(t)e^{\frac{-2x+x^2}{4Tv(t)}}\left(-\frac{I_1\left(\sqrt{c(t)(2x-x^2)}\right)}{\sqrt{c(t)(2x-x^2)}} + \frac{I_2\left(\sqrt{c(t)(2x-x^2)}\right)}{c(t)(2x-x^2)}\right), \tag{18}$$

$$p_2(t) = -\zeta(0,0,t) = \frac{1}{2}c(t). \tag{19}$$

Moreover

$$\sup_{0\le x\le y\le 1} |\zeta(x,y,t)| \le c_1 c(t) e^{\frac{\sqrt{\mu_0}}{v(t)}}. \tag{20}$$

The proof of Lemma 2 is presented in Appendix A.

The inverse transformation of (14) is given by

$$\begin{aligned}\eta(x,t) &= \phi(x,t) + \int_0^x \rho(x,y,t)\phi(y,t)\mathrm{d}y, \\ &:= [(I-\mathcal{R})^{-1}\phi](x,t),\end{aligned} \tag{21}$$

with the kernel function $\rho(x,y,t)$ satisfying

$$\begin{cases} \rho_{xx}(x,y,t) - \rho_{yy}(x,y,t) = \rho_t(x,y,t) + c(t)\rho(x,y,t), \\ \rho(x,x,t) = \frac{1}{2}c(t)(x-1), \\ \rho_x(1,y,t) = 0. \end{cases} \tag{22}$$

Lemma 3. *The solution to (22) is given by*

$$\rho(x,y,t) = -(1-y)c(t)e^{\frac{-(x-y)(2-x-y)}{4Tv(t)}} \frac{J_1\left(\sqrt{c(t)(x-y)(2-x-y)}\right)}{\sqrt{c(t)(x-y)(2-x-y)}}. \tag{23}$$

The proof of Lemma 3 is presented in Appendix B.

Using

$$\hat{\phi}(1,t) = D(t), \tag{24}$$

and evaluating (14) at $x = 1$, one obtains

$$\eta(1,t) = D(t) - \left(\varphi(1,t) - \int_0^1 \zeta(1,y,t)\eta(y,t)\,\mathrm{d}y\right). \tag{25}$$

Hence, $\eta(1,t)$ represents the disturbance estimation error.

If $|\eta(1,t)| \to 0$ as $t \to T$, then $\varphi(1,t) - \int_0^1 \zeta(1,y,t)\eta(y,t)\,\mathrm{d}y$ serves as a PT estimate of $D(t)$.

Lemma 4. *For any $\eta_0 \in \mathcal{H}$, system (16) admits a unique solution $\eta \in C([0,T);\mathcal{H})$ satisfying*

$$\|\eta(\cdot,t)\|_{\mathcal{H}} \le c_1 e^{-\frac{\mu_0 T}{v(t)}}. \tag{26}$$

If $\eta_0 \in H^1([0,1])$ satisfies the compatibility condition, then

$$|\eta(1,t)| \le c_1 e^{-\frac{\mu_0 T}{v(t)}}. \tag{27}$$

Proof. The well-posedness follows from Lemma 1. Consider

$$V_1(t) = \frac{1}{2}\|\eta(\cdot,t)\|_{\mathcal{H}}^2 + \frac{1}{2}\|\eta_x(\cdot,t)\|_{\mathcal{H}}^2.$$

Then,

$$\dot{V}_1(t) \le -c(t)\left(\|\eta(\cdot,t)\|_{\mathcal{H}}^2 + \|\eta_x(\cdot,t)\|_{\mathcal{H}}^2\right),$$

which implies (26). The boundary estimate follows from the Sobolev trace theorem $|\eta(1,t)| \le c_1(\|\eta(\cdot,t)\|_{\mathcal{H}} + \|\eta_x(\cdot,t)\|_{\mathcal{H}}) \le c_1 e^{\frac{-\mu_0 T}{v(t)}}$. □

Therefore, define

$$\hat{D}(t) = \varphi(1,t) - \int_0^1 \zeta(1,y,t)\eta(y,t)\,\mathrm{d}y, \quad \tilde{D}(t) = \eta(1,t).$$

Furthermore, the estimator also provides a state estimate

$$\hat{u}(x,t) = \phi(x,t) + \varphi(x,t),$$

and

$$\|\tilde{\phi}(\cdot,t)\|_{\mathcal{H}} \le c_1 c(t) e^{-\frac{a}{4Tv(t)}} \to 0 \quad \text{as } t \to T. \tag{28}$$

Remark 2. *Traditional backstepping employs time-invariant kernels and achieves exponential convergence as $t \to \infty$. In contrast, the time-varying kernel $\zeta(x,y,t)$ incorporates the gain $c(t) = \mu_0 T^2/(T-t)^2$, which diverges as $t \to T$, thereby enforcing convergence at the prescribed time T. In particular, the estimation error $\eta(1,t)$ vanishes at $t = T$, yielding PT disturbance estimation, whereas existing approaches only guarantee exponential convergence.*

3.2. Boundary Controller

To design the control input, we first transform the original system (1)–(3) into (30), which serves as the starting point for the PT stabilization design.

Consider the backstepping transformation with a time-invariant kernel

$$\begin{aligned}\vartheta(x,t) &= u(x,t) - \int_0^x p(x,y)u(y,t)\,\mathrm{d}y \\ &:= [(I-\mathcal{P})u](x,t),\end{aligned} \tag{29}$$

which shifts the destabilizing boundary term to the controlled boundary. The transformed system satisfies

$$\begin{cases} \vartheta_t = \vartheta_{xx}, \\ \vartheta_x(0,t) = 0, \\ \vartheta(1,t) = U(t) + D(t) - \int_0^1 p(1,y)u(y,t)\,\mathrm{d}y, \\ \vartheta(x,0) = \vartheta_0(x), \end{cases} \tag{30}$$

where $\vartheta_0(x) = u_0(x) - \int_0^x p(x,y)u_0(y)\,\mathrm{d}y$.

The kernel $p(x,y)$ satisfies

$$\begin{cases} p_{xx}(x,y) = p_{yy}(x,y) \\ p_y(x,0) = -qp(x,0) + \varrho e^{\alpha x} - \varrho \int_0^x p(x,y)e^{\alpha y}\mathrm{d}y, \\ p(x,x) = -q, \end{cases} \tag{31}$$

whose explicit solution is given as

$$p(x,y) = -e^{\frac{q+\alpha}{2}(x-y)}\left[q\cosh r(x-y) + \frac{2\varrho + q(q-\alpha)}{2r}\sinh r(x-y)\right], \tag{32}$$

with $r = \sqrt{\varrho + \frac{(\varrho-\alpha)^2}{4}}$.

The inverse transformation reads

$$\begin{aligned}u(x,t) &= \vartheta(x,t) + \int_0^x s(x,y)\vartheta(y,t)\,\mathrm{d}y \\ &:= [(I-\mathcal{P})^{-1}\vartheta](x,t),\end{aligned} \tag{33}$$

where $s(x,y)$ solves

$$\begin{cases} s_{xx}(x,y) = s_{yy}(x,y) \\ s_y(x,0) = \varrho e^{\alpha x}, \\ s(x,x) = -q, \end{cases} \tag{34}$$

whose explicit solution is explicitly given by

$$s(x,y) = \frac{\varrho}{\alpha}(1 - e^{\alpha(x-y)}) - q.$$

Hence, $s(x,y) \in C^\infty$ on $\{0 \le y \le x \le 1\}$, and $(I-\mathcal{P})^{-1}$ is bounded on $\mathcal{H}$.
Let

$$U(t) = U_0(t) + U_1(t), \quad U_0(t) = \int_0^1 p(1,y)u(y,t)\,\mathrm{d}y. \tag{35}$$

Substituting into (30) yields

$$\begin{cases} \vartheta_t = \vartheta_{xx}, \\ \vartheta_x(0,t) = 0, \vartheta(1,t) = U_1(t) + d(t), \\ \vartheta(x,0) = \vartheta_0(x). \end{cases} \tag{36}$$

Since time-invariant backstepping only ensures exponential stabilization, we proceed with a boundary time-varying feedback design (see [31,35]) to achieve PT convergence.
Introduce the transformation

$$\begin{aligned} \hat{\vartheta}(x,t) &= \vartheta(x,t) - \int_0^x \xi(x,y,t)\vartheta(y,t)\,\mathrm{d}y \\ &:= [(I-\mathcal{K})\vartheta](x,t), \end{aligned} \tag{37}$$

which yields

$$\begin{cases} \hat{\vartheta}_t = \hat{\vartheta}_{xx} - c(t)\hat{\vartheta}, \\ \hat{\vartheta}_x(0,t) = 0, \\ \hat{\vartheta}(1,t) = U_1(t) + d(t) - \int_0^1 \xi(1,y,t)\vartheta(y,t)\,\mathrm{d}y. \end{cases} \tag{38}$$

Applying the control law

$$U_1(t) = -\hat{D}(t) + \int_0^1 \xi(1,y,t)\vartheta(y,t)\,\mathrm{d}y, \tag{39}$$

one obtains

$$\begin{cases} \hat{\vartheta}_t = \hat{\vartheta}_{xx} - c(t)\hat{\vartheta}, \\ \hat{\vartheta}_x(0,t) = 0, \\ \hat{\vartheta}(1,t) = \tilde{D}(t) = \eta(1,t). \end{cases} \tag{40}$$

Define $\bar{\vartheta} = \hat{\vartheta} - \eta$, leading to

$$\begin{cases} \bar{\vartheta}_t = \bar{\vartheta}_{xx} - c(t)\bar{\vartheta}, \\ \bar{\vartheta}_x(0,t) = 0, \bar{\vartheta}(1,t) = 0, \end{cases} \tag{41}$$

which is a homogeneous stable system with PT convergence.
The kernel $\xi(x,y,t)$ satisfies

$$\begin{cases} \xi_{xx}(x,y,t) - \xi_{yy}(x,y,t) = \xi_t(x,y,t) + c(t)\xi(x,y,t), \\ \xi(x,x,t) = -\frac{1}{2}c(t)x, \\ \xi_y(x,0,t) = 0, \end{cases} \tag{42}$$

defined on the domain $\Xi = \{(x,y,t) \in R^2 \times [0,T) : 0 \le y \le x \le 1\}$, and its explicit expression is given in Lemma 5.

Lemma 5. *The solution of the problem (42) is given by*

$$\xi(x,y,t) = -xc(t)e^{\frac{(x^2-y^2)}{4Tv(t)}}\frac{I_1(\sqrt{c(t)(x^2-y^2)})}{\sqrt{c(t)(x^2-y^2)}}. \tag{43}$$

Moreover,

$$\sup_{0\le x\le y\le 1}|\xi(x,y,t)| \le c_1 c(t) e^{\frac{1+4T\sqrt{\mu_0}}{4Tv(t)}}. \tag{44}$$

The proof of Lemma 5 is presented in Appendix C.
The inverse transformation of (37) is defined by

$$\begin{aligned}\vartheta(x,t) &= \hat{\vartheta}(x,t) + \int_0^x \kappa(x,y,t)\hat{\vartheta}(y,t)\mathrm{d}y,\\ &:= [(I-\mathcal{K})^{-1}\hat{\vartheta}](x,t),\end{aligned} \tag{45}$$

with kernel $\kappa(x,y,t)$ formulated by

$$\begin{cases}\kappa_{xx}(x,y,t) - \kappa_{yy}(x,y,t) = \kappa_t(x,y,t) - c(t)\kappa(x,y,t),\\ \kappa(x,x,t) = -\frac{1}{2}c(t)x,\\ \kappa_y(x,0,t) = 0.\end{cases} \tag{46}$$

and characterized in Lemma 6.

Lemma 6. *The solution of the problem (42) is given by*

$$\kappa(x,y,t) = -xc(t)e^{\frac{(x^2-y^2)}{4Tv(t)}}\frac{J_1(\sqrt{c(t)(x^2-y^2)})}{\sqrt{c(t)(x^2-y^2)}}. \tag{47}$$

Furthermore,

$$\sup_{0\le y\le x\le 1}|\kappa(x,y,t)| \le c(t)e^{\frac{1}{4Tv(t)}} := M_\kappa(t). \tag{48}$$

The proof of Lemma 6 is presented in Appendix D.
Combining (35) and (39), the state feedback control law is obtained as

$$\begin{aligned}U(t) = &\int_0^1 p(1,y)u(y,t)\,\mathrm{d}y - \varphi(1,t)\\ &+\int_0^1 \zeta(1,y,t)[(I-\mathcal{R})^{-1}(u-\varphi-\phi)](y,t)\,\mathrm{d}y\\ &+\int_0^1 \xi(1,y,t)\Big(u(y,t) - \int_0^y p(y,h)u(h,t)\,\mathrm{d}h\Big)\mathrm{d}y.\end{aligned} \tag{49}$$

Replacing u by its estimate $\hat{u} = \phi + \varphi$, we obtain the output feedback controller

$$\begin{aligned}U(t) = &\int_0^1 p(1,y)(\phi+\varphi)\,\mathrm{d}y - \varphi(1,t)\\ &+\int_0^1 \xi(1,y,t)(\phi+\varphi)\,\mathrm{d}y\\ &-\int_0^1 \xi(1,y,t)\int_0^y p(y,h)(\phi+\varphi)\,\mathrm{d}h\,\mathrm{d}y.\end{aligned} \tag{50}$$

Remark 3. *The time-varying kernels admit explicit closed-form expressions. Hence, no online solution of kernel PDEs is required. In implementation, kernel values can be precomputed offline and stored, so that the controller reduces to evaluating algebraic expressions and spatial integrals, resulting in low computational complexity suitable for real-time applications.*

3.3. Closed-Loop System

Substituting (49) into (1)–(3) yields the closed-loop system

$$\begin{cases} u_t = u_{xx} + \varrho e^{\alpha x} u(0,t), \\ u_x(0,t) = -qu(0,t), \\ u(1,t) = \chi(u) + d(t) - \varphi(1,t) + \int_0^1 p(1,y)(\varphi+\phi)\,\mathrm{d}y \\ \qquad\quad + \int_0^1 \xi(1,y,t)(\varphi+\phi)\,\mathrm{d}y - \int_0^1 \xi(1,y,t)\int_0^y p(y,h)(\varphi+\phi)\,\mathrm{d}h\,\mathrm{d}y, \\ u(0) = u_0, \end{cases} \tag{51}$$

together with the auxiliary system

$$\begin{cases} \phi_t = \phi_{xx} + \varrho e^{\alpha x} u(0,t), \\ \phi_x(0,t) = 0, \\ \phi(1,t) = -\varphi(1,t) + \int_0^1 p(1,y)(\varphi+\phi)\,\mathrm{d}y \\ \qquad\quad + \int_0^1 \xi(1,y,t)(\varphi+\phi)\,\mathrm{d}y - \int_0^1 \xi(1,y,t)\int_0^y p(y,h)(\varphi+\phi)\,\mathrm{d}h\,\mathrm{d}y, \\ \phi(0) = \phi_0, \end{cases} \tag{52}$$

and the estimator

$$\begin{cases} \varphi_t = \varphi_{xx} - c(t)\varphi, \\ \varphi_x(0,t) = -p_2(t)\big(u(0,t) - \phi(0,t) - \varphi(0,t)\big), \\ \varphi_x(1,t) = u_x(1,t) - \phi_x(1,t), \\ \varphi(0) = \varphi_0. \end{cases} \tag{53}$$

Theorem 1. *Suppose $d \in L^\infty([0,T);\mathbb{R})$, $\chi : \mathcal{H} \to \mathbb{R}$ is continuous, and $T > 0$ is prescribed. For any $(u_0, \varphi_0, \phi_0) \in \mathcal{H}^3$, system (51)–(53) admits a unique solution $(u, \hat{u}, \varphi, \phi) \in C([0,T);\mathcal{H}^3)$. If $\sqrt{\mu_0} > \frac{1+\sqrt{3}}{2T}$, then*

$$\|u(\cdot,t)\|_{\mathcal{H}} \to 0, \quad t \to T,$$

and

$$\sup_{t\in[0,T)} \big(\|\varphi(\cdot,t)\|_{\mathcal{H}} + \|\phi(\cdot,t)\|_{\mathcal{H}}\big) < \infty.$$

Proof. Introduce the inverse transformation

$$\begin{pmatrix} u \\ \varphi \\ \phi \end{pmatrix} = \begin{pmatrix} (I-\mathcal{P})^{-1}(I-\mathcal{K})^{-1} & (I-\mathcal{P})^{-1}(I-\mathcal{K})^{-1} & 0 \\ 0 & -(I-\mathcal{R})^{-1} & I \\ (I-\mathcal{P})^{-1}(I-\mathcal{K})^{-1} & (I-\mathcal{P})^{-1}(I-\mathcal{K})^{-1} & -I \end{pmatrix} \begin{pmatrix} \bar{\vartheta} \\ \eta \\ \hat{\phi} \end{pmatrix}. \tag{54}$$

The equivalent system becomes

$$\begin{cases} \bar{\vartheta}_t = \bar{\vartheta}_{xx} - c(t)\bar{\vartheta}, \quad \bar{\vartheta}_x(0,t) = 0,\ \bar{\vartheta}(1,t) = 0, \\ \eta_t = \eta_{xx} - c(t)\eta, \quad \eta_x(0,t) = 0,\ \eta_x(1,t) = 0, \\ \hat{\phi}_t = \hat{\phi}_{xx}, \quad \hat{\phi}_x(0,t) = 0, \\ \hat{\phi}(1,t) = \chi\big([(I-\mathcal{P})^{-1}(I-\mathcal{K})^{-1}(\bar{\vartheta}+\eta)]\big) + d(t). \end{cases} \tag{55}$$

By Lemma 1, $(\bar{\vartheta}, \eta) \in C([0,T); \mathcal{H}^2)$ and

$$\|\bar{\vartheta}\|_{\mathcal{H}} + \|\eta\|_{\mathcal{H}} \le c_1 e^{-\frac{\mu_0 T}{\nu(t)}}. \tag{56}$$

Using the boundedness of $(I-\mathcal{P})^{-1}$ and (48),

$$\begin{aligned} \|u\|_{\mathcal{H}} &\le c_1(1 + M_\kappa(t))(\|\bar{\vartheta}\|_{\mathcal{H}} + \|\eta\|_{\mathcal{H}}) \\ &\le c_1 c(t) e^{-\frac{a}{4T\nu(t)}}. \end{aligned} \tag{57}$$

Hence, $\|u\| \to 0$ as $t \to T$ if $\sqrt{\mu_0} > \frac{1}{2T}$.

Since χ is continuous, $\chi(u) \in L^\infty([0,T))$, thus $D(t) = \chi(u) + d(t) \in L^\infty([0,T))$. Standard arguments (cf. Lemma 1) yield $\hat{\phi} \in C([0,T); \mathcal{H})$ and

$$\sup_{t\in[0,T)} \|\hat{\phi}\|_{\mathcal{H}} < \infty. \tag{58}$$

From $\varphi = \hat{\phi} - \phi$ and (56), (58), it follows that

$$\sup_{t\in[0,T)} \|\varphi\|_{\mathcal{H}} < \infty, \quad \sup_{t\in[0,T)} \|\phi\|_{\mathcal{H}} < \infty.$$

□

Lemma 7. *Under the assumptions of Theorem 1, for* $(u_0, \varphi_0, \phi_0) \in \mathcal{H}_a^3$ *and* $\sqrt{\mu_0} > \frac{1+\sqrt{3}}{2T}$, *the control input* (50) *satisfies*

$$\|U\|_{L^\infty([0,T))} < \infty.$$

Proof. Rewrite

$$U = U_a + U_b + U_c,$$

with

$$\begin{aligned} U_a &= \int_0^1 p(1,y)(u-\phi)\,\mathrm{d}y, \\ U_b &= -\varphi(1,t), \\ U_c &= \int_0^1 \xi(1,y,t)[(I-\mathcal{P})(u-\phi)]\,\mathrm{d}y. \end{aligned}$$

From (57),

$$\|u-\phi\|_{\mathcal{H}} \le c_1 c(t) e^{-\frac{a}{4T\nu(t)}}.$$

Hence,

$$|U_a| \le c_1 c(t) e^{-\frac{a}{4T\nu(t)}}, \quad |U_c| \le c_1 c^2(t) e^{-\frac{b}{4T\nu(t)}}.$$

Thus $U_a, U_c \in L^\infty([0,T))$.

Since $|U_b| \le |D(t)|$ and $D \in L^\infty$, one has $U_b \in L^\infty$. Therefore $U \in L^\infty([0,T))$. □

https://doi.org/10.3390/axioms15040257

Remark 4. *As pointed out in [31,36], PT stabilization of the heat equation subject to boundary disturbances such as $D(t)$ remains an open problem. The present work addresses this issue by allowing boundary disturbances at the actuated end, while simultaneously accommodating a destabilizing term at the uncontrolled boundary.*

Remark 5. *The prescribed convergence time T is independent of the initial condition by construction. From the proof of Theorem 1, the solution satisfies*

$$\|u(\cdot,t)\|_{L^2(0,1)} \leq c_1 e^{-\frac{a}{4Tv(t)}} \|u(\cdot,0)\|_{L^2(0,1)},$$

where $c_1, a > 0$. Since $\frac{a}{4Tv(t)} \to +\infty$ as $t \to T$, the exponential term vanishes, guaranteeing convergence at the prescribed time T. This also indicates reduced sensitivity with respect to the initial condition.

The controller design depends on the system parameters ρ, α, and q through the construction of the backstepping kernels, and the disturbance estimator relies on an auxiliary system parameterized by these quantities. The impact of parameter uncertainties on the transformation accuracy and estimation performance remains to be investigated.

Remark 6. *The proposed approach assumes that the disturbance $d(t)$ is bounded, which is consistent with most practical scenarios. If the disturbance varies faster than the convergence rate of the estimator, the estimation error may not decay sufficiently fast. Nevertheless, since the estimator gain $c(t)$ increases as $t \to T$, the estimator becomes increasingly responsive near the terminal time, partially compensating for such effects.*

Very large disturbances may cause actuator saturation or violate the underlying linear model assumptions. However, as established in Lemma 6, the control input remains bounded as $t \to T$, provided that $d(t)$ is bounded.

Remark 7. *The proposed control strategy admits a natural physical interpretation. The PT controller can be viewed as an accelerated cooling mechanism, where the time-varying gain $c(t)$ enhances the effective diffusion as $t \to T$, enforcing the temperature profile to vanish at the prescribed time.*

Although the gain becomes unbounded near T, the control input remains bounded due to the rapid decay of the system state. In addition, the disturbance estimator can be interpreted as a virtual sensor that reconstructs the unknown disturbance from boundary measurements within the prescribed time, thereby enabling effective compensation. As a result, the closed-loop system achieves convergence within a preassigned time independent of the initial condition.

4. Simulation

The solid propellant rocket is considered with the structural sketch shown in Figure 1 (see [4]). The temperature sensors are imposed at two boundary endpoints, measuring the temperature at $x = 0$ and the heat flux at $x = L$, respectively, while the control end is at $x = L$. The burning in solid rockets considered here is governed by (1)–(3) with $L = 1$ and $u(x,t)$ denoting the temperature. The finite difference method is used to run the simulation with the time step 0.001 and space step 0.05. For the corresponding closed-loop system (51)–(53), taking parameters $\alpha = 0$, $\varrho = 2$, $q = 1$, boundary total disturbance $D(t) = 2\sin(t) + 2\sin(u(0,t))$, initial values $u_0(x) = 0$, $\varphi_0(x) = 0.1(-2x + x^2)$, $\phi_0(x) = -0.4/\mu_0$, $\mu_0 = \frac{1+\sqrt{3}}{2} + 10$, respectively. The prescribed time is assumed to be $T = 1$ s.

The simulation results in Figures 2–7 demonstrate the effectiveness of the proposed estimator-based PT control scheme. As shown in Figure 2, the open-loop system exhibits unstable temperature growth due to the anti-stable dynamics. When the proposed controller

is applied (Figure 3), the temperature converges uniformly to zero as $t \to T$, indicating PT stabilization. Figure 4 further compares the convergence performance with the exponential stabilization method in [18], showing that the proposed controller drives the L^2-norm of the state to near zero exactly at the prescribed time, whereas the exponential controller converges only asymptotically. Figures 5 and 6 confirm that the disturbance estimator accurately reconstructs both the system state and the total disturbance within the prescribed time. Finally, Figure 7 illustrates that the convergence time remains T for different initial conditions, verifying that the PT property is independent of the initial state.

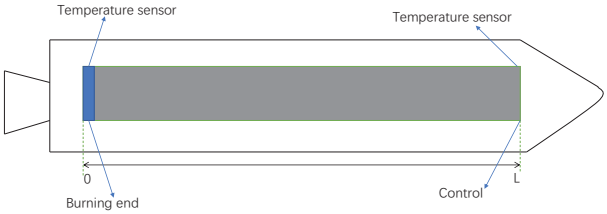


Figure 1. Solid propellant rocket.

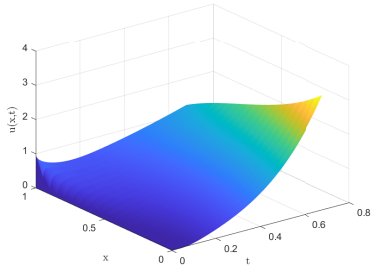


Figure 2. Open loop temperature $u(x,t)$.

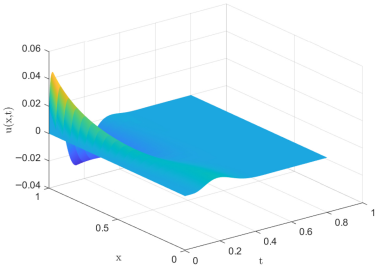


Figure 3. Temperature $u(x,t)$ under control.

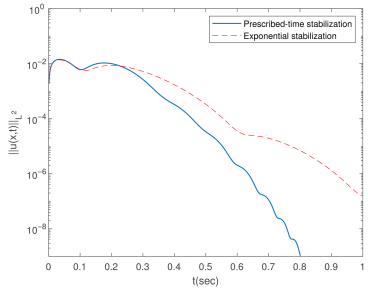


Figure 4. The L^2-norm of $u(x,t)$.

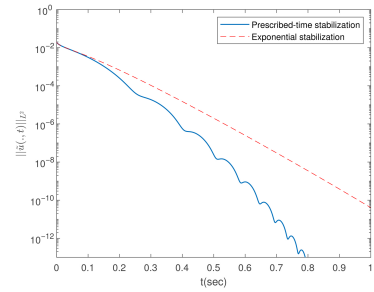


Figure 5. The L^2-norm of state estimator error $\tilde{u}(x,t)$.

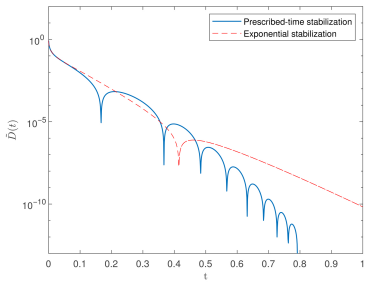


Figure 6. The L^2-norm of disturbance estimation error $\tilde{D}(t)$.

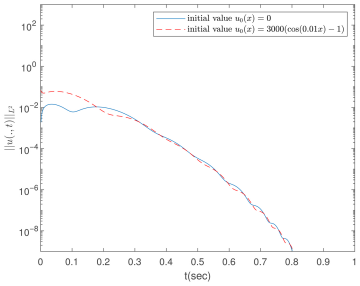


Figure 7. The evolution of $\|u(\cdot,t)\|_{L^2([0,1];R)}$ with different initial conditions $u_0(x) = 0$ (blue line), $u_0(x) = 3000(\cos(0.01x) - 1)$ (red line).

5. Conclusions

This paper addresses the PT stabilization problem for the heat equation subject to boundary-matched disturbances. The proposed control strategy ensures convergence within a user-assigned time that is independent of the initial condition. In addition, the developed disturbance observer enables accurate reconstruction of both the disturbance and the system state within the prescribed time.

The proposed framework is expected to be applicable to other distributed parameter systems, such as the linearized Schrödinger Equation [36] and coupled heat Equations [34], in the presence of boundary disturbances, which will be investigated in future work.

It is worth noting that, under the Dirichlet boundary condition $u(0,t) = 0$ (formally corresponding to $q \to +\infty$), the boundary measurement $u(0,t)$ is no longer available. This limitation necessitates the development of alternative control designs, which remains an open problem for future research.

Funding: This work was supported in part by the Zhejiang Provincial Natural Science Foundation of China under Grant No. LQN25A010027 and in part by the National Natural Science Foundation of China under Grant No. 12501622.

Data Availability Statement: All data generated or analyzed during this study are included in this published article.

Conflicts of Interest: The author declares that they have no known competing financial interests or personal relationships that could have appeared to influence the work reported in this paper.

Appendix A. Proof of Lemma 2

Proof. Following [32], introduce the change of variables

$$\bar{x} = 1 - x, \quad \bar{y} = 1 - y, \quad \bar{\zeta}(\bar{x}, \bar{y}, t) = \zeta(x, y, t).$$

Then, (15) is equivalently written as

$$\begin{cases} \bar{\zeta}_{\bar{x}\bar{x}} - \bar{\zeta}_{\bar{y}\bar{y}} = \bar{\zeta}_t - c(t)\bar{\zeta}, \\ \bar{\zeta}(\bar{x}, \bar{x}, t) = -\frac{1}{2}c(t)\bar{x}, \\ \bar{\zeta}_{\bar{x}}(0, \bar{y}, t) = 0. \end{cases}$$

Consider the transformation

$$\bar{\zeta}(\bar{x}, \bar{y}, t) = -\frac{\bar{y}}{2} e^{\int_0^t c(\tau)\mathrm{d}\tau} f(z, t), \quad z = \sqrt{\bar{y}^2 - \bar{x}^2}.$$

It follows that f satisfies

$$\begin{cases} f_t = -f_{zz} - \frac{3}{z} f_z, \\ f_z(0, t) = 0, \\ f(0, t) = c(t) e^{-\int_0^t c(\tau)\mathrm{d}\tau} =: G(t). \end{cases}$$

To handle the backward diffusion structure, introduce $\varsigma = T - t$ and define $f(z, t) = g(z, \varsigma)$. Then,

$$\begin{cases} g_\varsigma = g_{zz} + \frac{3}{z} g_z, \\ g_z(0, \varsigma) = 0, \\ g(0, \varsigma) = G(t). \end{cases}$$

The solution admits the series representation

$$g(z, \varsigma) = \sum_{n=0}^{\infty} \frac{z^{2n}}{4^n n!(n+1)!} g^{(n)}(0, \varsigma) = \sum_{n=0}^{\infty} \frac{(\bar{x}^2 - \bar{y}^2)^n}{4^n n!(n+1)!} G^{(n)}(t),$$

where $G^{(n)}(t) = \frac{d^n}{dt^n} G(t)$ denotes the nth time derivative, its explicit expression is provided in [31]

$$G^{(n)}(t) = \frac{(\sqrt{c(t)})^n}{(T\sqrt{\mu_0})^n} n! L_n^{(1)}((T\sqrt{\mu_0})c^{1/2}(t)) c(t) e^{-\int_0^t c(\tau)d\tau}. \tag{A1}$$

Here $L_n^1(\cdot)$ is the generalized Laguerre polynomial [47].
Using the Laguerre polynomial identity (see [31,47]),

$$\sum_{n=0}^{\infty} \frac{v^n L_n^1(\lambda)}{\Gamma(n+2)} = (vh)^{-1/2} e^v J_1(2\sqrt{v\lambda})$$

associated with $\Gamma(n+2) = (n+1)!$, $I_1(\varphi) = \frac{1}{\sqrt{-1}} J_1(\sqrt{-1}\lambda)$, one obtains

$$f(z, t) = 2c(t) e^{-\int_0^t c(\tau)\mathrm{d}\tau} e^{\frac{\bar{x}^2 - \bar{y}^2}{4Tv(t)}} \frac{I_1\left(\sqrt{c(t)(\bar{y}^2 - \bar{x}^2)}\right)}{\sqrt{c(t)(\bar{y}^2 - \bar{x}^2)}}.$$

This establishes (17). The growth bound (20) follows from the integral representation of $I_1(h) = \frac{1}{\pi}\int_0^\pi e^{h\cos(\theta)}\cos(\theta)d\theta$. □

Appendix B. Proof of Lemma 3

Proof. Applying the same transformation as Appendix A yields

$$\begin{cases} \bar{\rho}_{\bar{x}\bar{x}} - \bar{\rho}_{\bar{y}\bar{y}} = \bar{\rho}_t + c(t)\bar{\rho}, \\ \bar{\rho}(\bar{x},\bar{x},t) = -\frac{1}{2}c(t)\bar{x}, \\ \bar{\rho}_{\bar{x}}(0,\bar{y},t) = 0. \end{cases}$$

Let

$$\bar{\rho} = -\frac{\bar{y}}{2}e^{-\int_0^t c(\tau)\mathrm{d}\tau} f(z,t),$$

Then, f satisfies

$$\begin{cases} f_t = -f_{zz} - \frac{3}{z}f_z, \\ f_z(0,t) = 0, \\ f(0,t) = c(t)e^{\int_0^t c(\tau)\mathrm{d}\tau} =: F(t). \end{cases}$$

Using the expression of

$$F^{(n)}(t) = \frac{(\sqrt{\tilde{c}(t)})^n}{(T\sqrt{\tilde{\mu}_0})^n} n! L_n^{(1)}(-(T\sqrt{\tilde{\mu}_0})\tilde{c}^{1/2}(t))\tilde{c}(t)e^{\int_0^t \tilde{c}(\tau)d\tau} \tag{A2}$$

and proceeding as in Appendix A, one obtains (23). □

Appendix C. Proof of Lemma 5

Proof. Let $\bar{x} = y$, $\bar{y} = x$, $\bar{\xi}(\bar{x},\bar{y},t) = \xi(x,y,t)$. Then,

$$\begin{cases} \bar{\xi}_{\bar{x}\bar{x}} - \bar{\xi}_{\bar{y}\bar{y}} = -\bar{\xi}_t - c(t)\bar{\xi}, \\ \bar{\xi}(\bar{x},\bar{x},t) = -\frac{1}{2}c(t)\bar{x}, \\ \bar{\xi}_{\bar{x}}(0,\bar{y},t) = 0. \end{cases}$$

Seek a solution of the form

$$\bar{\xi} = -\frac{\bar{y}}{2}e^{-\int_0^t c(\tau)\mathrm{d}\tau} f(z,t),$$

which yields

$$\begin{cases} f_t = f_{zz} + \frac{3}{z}f_z, \\ f_z(0,t) = 0, \\ f(0,t) = c(t)e^{\int_0^t c(\tau)\mathrm{d}\tau} =: F(t). \end{cases}$$

The series representation follows as

$$f(z,t) = \sum_{n=0}^{\infty} \frac{(\bar{y}^2 - \bar{x}^2)^n}{4^n n!(n+1)!} F^{(n)}(t),$$

where $F^{(n)}$ is given in (A2). The result (43) and bound (44) follow analogously to Appendix A. □

Appendix D. Proof of Lemma 6

Proof. Introduce the change of variables

$$\bar{x} = y, \quad \bar{y} = x, \quad \bar{\kappa}(\bar{x}, \bar{y}, t) = \kappa(x, y, t).$$

Then, the system is equivalently written as

$$\begin{cases} \bar{\kappa}_{\bar{x}\bar{x}} - \bar{\kappa}_{\bar{y}\bar{y}} = -\bar{\kappa}_t + c(t)\bar{\kappa}, \\ \bar{\kappa}(\bar{x}, \bar{x}, t) = -\frac{1}{2}c(t)\bar{x}, \\ \bar{\kappa}_{\bar{x}}(0, \bar{y}, t) = 0. \end{cases}$$

Consider the transformation

$$\bar{\kappa}(\bar{x}, \bar{y}, t) = -\frac{\bar{y}}{2} e^{\int_0^t c(\tau)\mathrm{d}\tau} f(z, t), \quad z = \sqrt{\bar{y}^2 - \bar{x}^2}.$$

It follows that f satisfies

$$\begin{cases} f_t = f_{zz} + \frac{3}{z} f_z, \\ f_z(0, t) = 0, \\ f(0, t) = c(t) e^{-\int_0^t c(\tau)\mathrm{d}\tau} =: G(t). \end{cases}$$

The $G^{(n)}(t)$ is given in (A1). Proceeding as in Lemma 2, one obtains (47) and the bound (48). □

References

1. Mao, D.; Jiang, G.; Ye, Q.; Chen, M. Synchronization of Networked Reaction-Diffusion Nonlinear Systems via Hybrid Control. *Axioms* **2025**, *14*, 885. [CrossRef]
2. Qu, L.; Jiang, Z.; Wu, L. Color Image Storage and Retrieval via Sliding Mode Control of Quaternion-Valued Neural Networks. *Axioms* **2026**, *15*, 72. [CrossRef]
3. Xie, Y.; Tian, C.; Li, Y. Exponential Stability of a Wave Equation with Boundary Delay Control. *Axioms* **2025**, *14*, 280. [CrossRef]
4. Boskovic, D.M.; Krstic, M. Stabilization of a solid propellant rocket instability by state feedback. *Int. J. Robust Nonlinear Control* **2003**, *13*, 483–495. [CrossRef]
5. Smyshlyaev, A.; Krstic, M. Closed-form boundary state feedbacks for a class of 1-D partial integro-differential equations. *IEEE Trans. Autom. Control* **2004**, *49*, 2185–2202. [CrossRef]
6. Liu, J.J.; Wang, J.M. Active disturbance rejection control and sliding mode control of one-dimensional unstable heat equation with boundary uncertainties. *IMA J. Math. Control Inf.* **2015**, *32*, 97–117. [CrossRef]
7. Cheng, M.B.; Radisavljevic, V.; Su, W.C. Sliding mode boundary control of a parabolic PDE system with parameter variations and boundary uncertainties. *Automatica* **2011**, *47*, 381–387. [CrossRef]
8. Kang, W.; Guo, B.Z. Lyapunov approach to boundary stabilization of an anti-stable heat equation with boundary disturbance. In Proceedings of the 33rd Chinese Control Conference, Nanjing, China, 28–30 July 2014.
9. Dai, J.; Ren, B. UDE-based robust boundary control for an unstable parabolic PDE with unknown input disturbance. *Automatica* **2018**, *93*, 363–368. [CrossRef]
10. Krstic, M.; Smyshlyaev, A. *Boundary Control of PDEs: A Course on Backstepping Designs*; SIAM: Philadelphia, PA, USA, 2008.
11. Orlov, Y.V. *Discontinuous Systems: Lyapunov Analysis and Robust Synthesis Under Uncertainty Conditions*; Springer: London, UK, 2008.
12. Cheng, M.B.; Radisavljevic, V.; Su, W.C. Output-feedback boundary control of an uncertain heat equation with noncollocated observation: A sliding-mode approach. In Proceedings of the 2010 5th IEEE Conference on Industrial Electronics and Applications, Taichung, Taiwan, 15–17 June 2010.
13. Loudahi, L.; Yuan, J.; Dehbi, L.; Osman, M. Stabilization and Synchronization of a New 3D Complex Chaotic System via Adaptive and Active Control Methods. *Axioms* **2025**, *14*, 383. [CrossRef]
14. Smyshlyaev, A.; Krstic, M. Adaptive boundary control for unstable parabolic PDEs—Part III: Output feedback examples with swapping identifiers. *Automatica* **2007**, *43*, 1557–1564. [CrossRef]
15. Smyshlyaev, A.; Krstic, M. *Adaptive Control of Parabolic PDEs*; Princeton University Press: Princeton, NJ, USA, 2010.

16. Homayounzade, M. Adaptive robust output-feedback boundary control of an unstable parabolic PDE subjected to unknown input disturbance. *Int. J. Syst. Sci.* **2021**, *52*, 2324–2337. [CrossRef]
17. Han, J. From PID to active disturbance rejection control. *IEEE Trans. Ind. Electron.* **2009**, *56*, 900–906. [CrossRef]
18. Feng, H.; Guo, B.Z. New unknown input observer and output feedback stabilization for uncertain heat equation. *Automatica* **2017**, *86*, 1–10. [CrossRef]
19. Bhat, S.P.; Bernstein, D.S. Finite-time stability of continuous autonomous systems. *SIAM J. Control Optim.* **2000**, *38*, 751–766. [CrossRef]
20. Pisano, A.; Orlov, Y.; Usai, E. Tracking control of the uncertain heat and wave equation via power-fractional and sliding-mode techniques. *SIAM J. Control Optim.* **2011**, *49*, 363–382. [CrossRef]
21. Li, T.; Zhao, R.; Chen, C.P.; Fang, L.; Liu, C. Finite-time formation control of under-actuated ships using nonlinear sliding mode control. *IEEE Trans. Cybern.* **2018**, *48*, 3243–3253.
22. Wang, J.L.; Zhang, X.X.; Wu, H.N.; Huang, T.; Wang, Q. Finite-time passivity and synchronization of coupled reaction-diffusion neural networks with multiple weights. *IEEE Trans. Cybern.* **2018**, *49*, 3385–3397.
23. Wei, C.; Li, J. Finite-time non-fragile boundary feedback control for a class of nonlinear parabolic systems. *Nonlinear Dyn.* **2021**, *103*, 2753–2768. [CrossRef]
24. Yang, S.; He, H.; Leung, M.F.; Tang, Y.; Yan, L. Fast Fixed-Time Control for Intra- and Inter-Layer Synchronization of Multi-Layer Networks. *Axioms* **2025**, *14*, 795. [CrossRef]
25. Chitre, R.; Haddad, W.M. Finite Time Stability and Optimal Control for Stochastic Dynamical Systems. *Axioms* **2025**, *14*, 767. [CrossRef]
26. Polyakov, A. Nonlinear feedback design for fixed-time stabilization of linear control systems. *IEEE Trans. Autom. Control* **2011**, *57*, 2106–2110. [CrossRef]
27. Polyakov, A.; Efimov, D.; Perruquetti, W. Finite-time and fixed-time stabilization: Implicit Lyapunov function approach. *Automatica* **2015**, *51*, 332–340. [CrossRef]
28. Wang, G.; Mamtimin, I.; Abdurahman, A. Fixed/Predefined-Time Synchronization for Delayed Memristive Reaction-Diffusion Neural Networks Subject to Stochastic Disturbances. *Axioms* **2026**, *15*, 209. [CrossRef]
29. Abudireman, A.; Abdurahman, A.; Jiang, H. Fixed-Time Synchronization of Spatiotemporal Cohen–Grossberg Neural Networks via Aperiodic Intermittent Control. *Commun. Nonlinear Sci. Numer. Simul.* **2025**, *150*, 108991. [CrossRef]
30. Song, Y.; Wang, Y.; Holloway, J.; Krstic, M. Time-varying feedback for regulation of normal-form nonlinear systems in prescribed finite time. *Automatica* **2017**, *83*, 243–251. [CrossRef]
31. Espitia, N.; Polyakov, A.; Efimov, D.; Perruquetti, W. Boundary time-varying feedbacks for fixed-time stabilization of constant-parameter reaction-diffusion systems. *Automatica* **2019**, *103*, 398–407. [CrossRef]
32. Smyshlyaev, A.; Krstic, M. On control design for PDEs with space-dependent diffusivity or time-dependent reactivity. *Automatica* **2005**, *41*, 1601–1608. [CrossRef]
33. Coron, J.M.; Nguyen, H.M. Null controllability and finite time stabilization for the heat equations with variable coefficients in space in one dimension via backstepping approach. *Arch. Ration. Mech. Anal.* **2017**, *225*, 993–1023. [CrossRef]
34. Espitia, N.; Polyakov, A.; Efimov, D.; Perruquetti, W. On continuous boundary time-varying feedbacks for fixed-time stabilization of coupled reaction-diffusion systems. In Proceedings of the 2018 IEEE Conference on Decision and Control (CDC), Miami, FL, USA, 17–19 December 2018.
35. Steeves, D.; Krstic, M.; Vazquez, R. Prescribed-time H^1-stabilization of reaction-diffusion equations by means of output feedback. In Proceedings of the 2019 18th European Control Conference (ECC), Napoli, Italy, 25–28 June 2019.
36. Steeves, D.; Krstic, M.; Vazquez, R. Prescribed-time estimation and output regulation of the linearized Schrödinger equation by backstepping. *Eur. J. Control* **2020**, *55*, 3–13. [CrossRef]
37. Steeves, D.; Camacho-Solorio, L.; Krstic, M. Boundary prescribed-time stabilization of a pair of coupled reaction-diffusion equations. In Proceedings of the 2020 American Control Conference (ACC), Denver, CO, USA, 1–3 July 2020.
38. Wei, C.; Li, J. Prescribed-Time Stabilization of Semi-Linear Parabolic Equations Subject to Distributed Disturbance. *ISA Trans.* **2021**, *128*, 355–366. [CrossRef] [PubMed]
39. Wei, C.; Li, J. Prescribed-Time Stabilization of Uncertain Heat Equation with Dirichlet Boundary Control. *IMA J. Math. Control Inf.* **2023**, *40*, 1471–1487. [CrossRef]
40. Wei, C.; Li, J.; He, C. Prescribed-Time Stabilisation for Uncertain Reaction-Diffusion Equations with Neumann Boundary Control. *Int. J. Control* **2023**, *96*, 2374–2383. [CrossRef]
41. Wei, C.; Li, J. Prescribed-Time Stabilization of Uncertain Heat Equation via Boundary Time-Varying Feedback and Disturbance Estimator. *Syst. Control Lett.* **2023**, *171*, 105419. [CrossRef]
42. Wei, C.; Xia, Z. Prescribed-Time and Output Feedback Stabilization of Heat Equation with an Intermediate-Point Heat Source and Boundary Control. *Syst. Control Lett.* **2024**, *192*, 105891. [CrossRef]

43. Li, M.; Long, Y.; Zhang, K.; Li, T. Time-varying dynamic event-triggered-based prescribed-time leader-following consensus for multi-agent systems with input saturation. *Appl. Math. Comput.* **2026**, *508*, 129630. [CrossRef]
44. Kong, Y.; Mao, B.; Wu, X.; Feng, J.; Huang, T. Predefined-time exact tracking for nonstrict feedback nonlinear systems: A novel switching feedback gain method. *IEEE Trans. Syst. Man Cybern. Syst.* **2026**.
45. Zeng, X.; Hua, C.; Li, K. Robust Composite Adaptive Predefined-Time Control of n-Link Robotic Systems with Prescribed Performance. *Sci. China Inf. Sci.* **2026**, *69*, 132201. [CrossRef]
46. Zekraoui, S.; Espitia, N.; Perruquetti, W.; Krstic, M. Output-Feedback Stabilization in Prescribed-Time of a Class of Reaction-Diffusion PDEs With Boundary Input Delay. *IEEE Trans. Autom. Control* **2025**, *70*, 5066–5081. [CrossRef]
47. Szego, G. *Orthogonal Polynomials*; American Mathematical Society: Providence, RI, USA, 1975; Volume 23.
48. Denison, M.R.; Baum, E. A Simplified Model of Unstable Burning in Solid Propellants. *ARS J.* **1961**, *31*, 1112–1122. [CrossRef]

Disclaimer/Publisher's Note: The statements, opinions and data contained in all publications are solely those of the individual author(s) and contributor(s) and not of MDPI and/or the editor(s). MDPI and/or the editor(s) disclaim responsibility for any injury to people or property resulting from any ideas, methods, instructions or products referred to in the content.